Influence of reference tube location on the measured sodium concentrations in calf muscles using a birdcage coil at 3T

Baron, Paul; Potze, Jan Hendrik; Sijens, Paul E.

Published in:
Magnetic resonance in medicine

DOI:
10.1002/mrm.29670

Received: 13 January 2023 | Revised: 17 March 2023 | Accepted: 26 March 2023 | Published on: 24 April 2023

DOI: 10.1002/mrm.29670

Magnetic Resonance in Medicine

TECHNICAL NOTE

Influence of reference tube location on the measured sodium concentrations in calf muscles using a birdcage coil at 3T

Paul Baron | **Jan Hendrik Potze** | **Paul E. Sijens**

Department of Radiology, University Medical Center Groningen, University of Groningen, Groningen, The Netherlands

Correspondence
Paul Baron, Department of Radiology, University of Groningen, University Medical Center Groningen, Hanzeplein 1, 9713 GZ Groningen, the Netherlands.
Email: p.baron@umcg.nl

Purpose: To investigate the influence of the sodium (Na) reference tube location in a birdcage coil on the quantification of Na in the calf muscle. Two correction methods were also evaluated.

Method: Eight (4×20 mM, 4×30 mM Na) reference tubes were placed along the inner surface of the coil and one (30 mM Na) tube more centrally near the tibia. In two volunteers, four repeated UTE scans were acquired. In six calf muscles, the Na concentration was calculated based on each reference tube. Flip angle mapping of a homogenous Na phantom was used for correcting intensity values. Alternatively, a normalized intensity map was used for correcting the in vivo signal intensities. Results were given as range or SD of Na concentration measurements over the reference tubes.

Results: For calf Na measurements, there was limited space for positioning reference tubes away from coil B_1 inhomogeneity. In both volunteers, the Na quantification depended greatly on the reference tube used with a range of up to 10 mM. The central tube location gave a Na quantification close to the mean of the other tubes. The flip angle and normalized signal intensity phantom-based correction methods decreased the quantification variation from 14.9% to 5.0% and 10.4% to 2.7%, respectively. Both correction methods had little influence ($< 2.3\%$) on quantification based on the central tube.

Conclusion: Despite use of a birdcage coil, location of the reference tube had a great impact on Na quantification in the calf muscles. Although both correction methods did reduce this variation, placing the reference tube more centrally was found to give the most reliable results.

KEYWORDS

calf muscle, reproducibility, sodium quantification

1 | INTRODUCTION

Sodium (Na) electrolyte homeostasis in the human body plays an important role in the physiology and pathophysiology of many diseases.[1] Na MRI has shown potential to probe these pathologies in the clinical setting. Areas include the brain such as tumors,[2] multiple sclerosis,[3] cartilage of the knee,[4] and kidney.[5] Increased total Na concentration measured in the calf muscle by MRI was found to be related to patients with refractory hypertension[6] and diabetes.[7] In addition, Na MRI of skeletal muscle utilizing an inversion pulse was found to be especially sensitive to the condition of muscular channelopathies.[8]

The required sensitivity of the Na measurements in leg muscle will depend on the disease or process being examined. For example, a mean difference of 6 mM ^{23}Na was found in the leg muscle between a group with diabetes and controls.[7] A mean elevated ^{23}Na signal in leg muscles of 2.2 mM was found during anaerobic exercise.[9]

Most Na MRI imaging studies of the skeletal muscle concentrate on obtaining an as homogeneous as possible B_0 field by shimming on the hydrogen (^{1}H) signals but do not correct for B_1 inhomogeniety. This could be due to increased acquisition time[10] required for B_1 mapping, or because a comparatively homogenous B_1 field was measured in a phantom when using a birdcage coil.[10,11] The birdcage coil design is known to have a highly homogenous B_1 field.[12] Due to the low signal received from Na (3000–20,000 lower[13]) compared to proton, the smallest possible coil diameter producing a homogeneous B_1 field is desirable. However, B_1 inhomogeniety in a tight-fitting birdcage coil has been implicated for an elevated Na signal when the leg is too close to the active RF coil elements.[14]

The aim of this study was to investigate and quantify the influence of the location of the Na reference tubes on the measured Na concentration in the muscles when using a birdcage coil. Additionally, two methods to correct for the coil B_1 inhomogeneity were evaluated.

2 | METHODS

2.1 | Na UTE MR imaging

In this study, UTE scans were acquired with a 3D density-adapted radial UTE sequence (DA-UTE)[15] on a Skyra 3T system (Siemens, Erlangen, Germany). The following settings were used for all UTE scans: TE = 0.2 ms, number of radial projections = 5000, readout duration = 20 ms, duration of radial part = 0.5 ms, gradient strength = 3.68 mT/m, receiver bandwidth = 50 Hz/Pixel, volume = $329 \times 329 \times 329$ mm^3, matrix size (N) = $66 \times 66 \times 66$, nominal voxel size = $5.0 \times 5.0 \times 5.0$ mm^3, number of signal averages = 1. For the in vivo study: TR = 120 ms, flip angle (FA) = 90°, and acquisition time for one scan = 10 min 0 s. For the phantom experiment: TR = 300 ms, FA = 90° or 45°, and the acquisition time for one scan = 25 min 0 s.

For the anatomical overlay, one 2D gradient echo image was acquired from the ^{1}H channel with parameters: TE = 3.7 ms, TR = 8.6 ms, flip angle (FA) = 20°, FOV = 250 mm^2, matrix size = 256×256, slice thickness = 7 mm, and number of signal averages = 2.

For signal transmit/receive a dual ^{23}Na/^{1}H birdcage knee coil (RAPID Biomedical, Rimpar, Germany; inner diameter = 18 cm) was used. For the in vivo scan of the calf muscle, the volunteer was in supine position, with the scanned leg and coil positioned in the center of the bore of the scanner.

Every scan session started with calibrating the reference voltage of the Na signal using an automated nonselective free induction decay B_1 mapping sequence. Then, a dummy single-voxel spectroscopy scan with the adjustment volume containing the whole tissue or phantom region was used to shim on the ^{1}H signal. The shim settings and reference voltage were then copied to the DA-UTE sequence, and the demodulation frequency of Na was manually adjusted prior to scanning.

2.2 | FA mapping of coil

To evaluate the homogeneity of the B_1 field within the axial field of the coil, FA maps were acquired in the axial plane of a large spherical (d = 18 cm; 100 mM Na $C_2H_3O_2$) quality-assurance phantom (Figure 1(A)). The imaging parameters of the DA-UTE sequence used are given in the section 2.1 with TR = 300 ms. The actual FA (α_{45}), assuming nominal 45°, was calculated with the double angle method[16] using images acquired with FAs of 45° (I_{45}) and 90° (I_{90}) of consecutively acquired scans as

$$\alpha_{45} = \arccos\left(\left| \frac{I_{90}}{2\, I_{45}} \right| \right). \quad (1)$$

The homogenous region for which the FA error = $|\, \alpha_{45} - 45° \,| < 10°$ was determined and compared to the position of the leg and reference tubes as acquired with the localizer.

2.3 | Measured muscle concentration dependence on reference tube position

To evaluate the dependence of the measured muscle concentration on the reference tube location, four tubes (diameter = 25 mm) with 20 mM sodium chloride (NaCl) saline solution were positioned along the left hand side

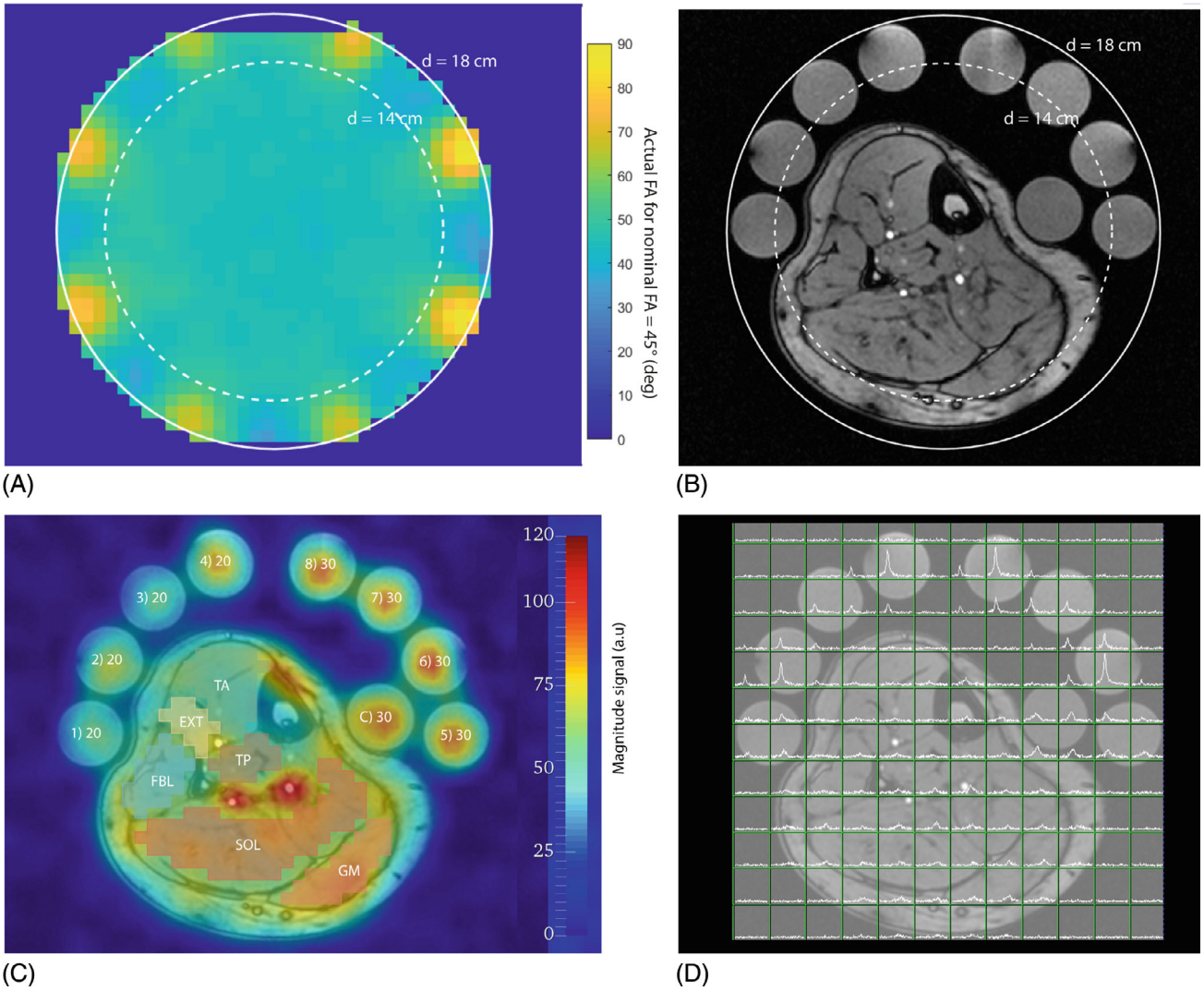

FIGURE 1 (A) FA map for the UTE acquisition with nominal FA = 45°. (B) Corresponding axial localizer image, with outer circle (solid line) indicating inner diameter of coil. The smaller circle (dashed line) indicates FA error < 10° (FA nominal = 45°) within its region. (C) Example image of the UTE signal overlay on the axial localizer image. Position of the tubes are shown with tubes 1–4 containing 20 mM NaCl and tubes 5–8 and central tube C containing 30 mM NaCl. Example ROIs drawn in the muscle groups are also shown. (D) The spectral map. FA, flip angle; NaCl, sodium chloride; ROI, region of interest.

of the coil surface (Figure 1(C)), and another four tubes with 30 mM NaCl solution on the right side. An additional 30 mM NaCl solution was positioned more centrally in the cavity near the tibia (Figure 1(C)). Two different tube NaCl concentrations were used to compare the results using different Na concentrations with the range expected in calf muscle.

Two volunteers were scanned in total. This work involving human subjects was conducted with informed consent and approval of the institutional review board. First, a localizer was acquired in three orthogonal orientations of the lower leg; then, this was followed by four repeated DA-UTE (FA = 90°, TR = 120 ms) scans to evaluate the intrascan session reproducibility of the concentration measurements.

For the in vivo study, a lower TR was used than for the phantom experiments in order to reduce the total acquisition time to a more acceptable duration. However, the smaller TR with respect to the Na-T_1 of saline solution of about $T_{1saline} = 54$ ms at 20°C[8] of the reference tubes does imply that T_1 saturation will occur. Given that the Na-T_1 of muscle ($T_{1muscle}$) as measured at 4T and 7T is about 25 ms,[17,18] a simple correction factor (T_{1cor}) was applied to the intensity of the reference tubes prior to calculating the concentrations of the muscle:

$$T_{1cor} = \frac{\left(1 - \exp\left(-\frac{TR}{T_{1muscle}}\right)\right)}{\left(1 - \exp\left(-\frac{TR}{T_{1saline}}\right)\right)} = \frac{\left(1 - \exp\left(-\frac{120}{25}\right)\right)}{\left(1 - \exp\left(-\frac{120}{54}\right)\right)} \approx 1.11. \quad (2)$$

For both volunteers and all four repeated measurements, the mean UTE signal (I_{muscle}) in the muscles—tibialis anterior (TA), extensor longus, tibialis posterior, fibularis, soleus, and gastrocnemius medialis (GM)—were measured by using the UTE image overlay on the axial localizer and drawing regions of interest (Figure 1(C)) in the muscles groups using 3D slicer[19] (www.slicer.org). Similarly the maximum UTE signal ($I_{max\ tube}$) within each of the nine tubes were measured. The maximum signal was used for the reference tubes to avoid partial volume effects with air. The concentration in one muscle group, using the 20 or 30 mM NaCl reference tube, was then calculated assuming a linear concentration–UTE signal relationship and UTE signal of 0 at 0 mM NaCl as:

$$C_{m=}C_{tube}\frac{I_{muscle}}{T_{1cor}\ I_{max\ tube}}. \quad (3)$$

Where C_{tube} is equal to 20 or 30 mM depending on the tube used for the calibration, and $I_{max\ tube}$ is the corresponding maximum UTE signal within the tube.

Na MRS measurement was performed additionally purely to illustrate an alternative way to visualize our Na imaging method. It involved 2D chemical shift imaging of an axial slice of 2.5 cm thickness and a FOV of $24\times24\ cm^2$ subdivided into 16×16 voxels of $15\times15\times25\ mm^3$ each. Free induction decay signals of FA 90° were acquired at TR/TE = 1500/2.3 ms and Fourier transformed to obtain the spectral map depicted in Figure 1(D).

2.4 | Correction in a phantom using a normalized FA map

To evaluate the effectiveness of FA correction, the homogenous phantom and FA = 45°/90° images described in the section 2.2 were also used for B_1 correction of the FA = 90° acquisition.

Firstly, given that this was a homogeneous spherical phantom and a hard pulse was used for UTE, the actual FA was assumed to be proportional to the average b_1^+[20]:

$$\alpha \propto b_1^+. \quad (4)$$

Following the principle of reciprocity in which the transmit and receive fields are assumed to be equal,[21] the coil sensitivity of the acquired magnitude image with nominal FA = 90° (I_{90}) was calculated as the actual FA with nominal 90° ($\propto_{90}$) divided by 90° ($\propto_{90}/90°$). The first corrected image ($I_{90\_receive\_cor}$) was therefore obtained by multiplying the I_{90} image by the inverse of the normalized FA map.

A second correction was applied to account for transmit FA errors. The FA error was assumed to scale with FA, and thus the actual FA with nominal 90° was calculated: $\propto_{90} = 90°\times(\propto_{45}/45°)$. The final corrected image (I_{90_cor}) was then obtained from:

$$I_{90\_cor} = \frac{I_{90\_receive\_cor}}{sin\ (\propto_{90})}. \quad (5)$$

To evaluate the effectiveness of the correction, similar positions were evaluated as the 30 mM tubes used for the in vivo scans. The intensity percent of these locations with respect to a (6×6 pixel) region of interest in the center of the phantom (as measured before the correction) was compared before and after B_1 correction.

2.5 | Correction using a normalized intensity map

The FA = 90° UTE scan of the homogeneous Na sphere (see section 2.2) was evaluated for its potential to correct for the coil B_1 inhomogeneity of the in vivo scan for volunteer 1. Firstly, the image of the phantom was normalized with respect to the mean of the central 6×6 pixel region assumed not to be affected by coil inhomogeneity.

Because the absolute position of the coil in the scanner with the phantom scanned may be different than the in vivo scan, the phantom image had to be shifted. In our specific case, the in vivo reference tubes were positioned at positions of maximum and minimum B_1 inhomogeneity. Therefore, the corrected image, given by the in vivo scan multiplied by the inversion of the normalized phantom image, was shifted such that the SD of both intensity-corrected 20 mM and 30 mM NaCl reference tube groups were minimized. Two assumptions were made—that the coil inhomogeneity is the same throughout the axial direction of the coil and that there is no coil rotation between the phantom and in vivo scan.

The correction was evaluated for the 30 mM tubes, and given as a percent of the intensity with respect to the 30 mM tube located more centrally, prior to the correction.

3 | RESULTS

3.1 | FA mapping of coil axial plane

Figure 1A shows the FA map ($FA_{nom} = 45°$) of one axial slice of the coil region. A homogenous B_1 region within the central circle of 14 cm diameter was found. When compared to the localizer scan of volunteer 1 (Figure 1B), the leg muscles are entirely in the homogeneous region. All reference tubes along the surface of the coil are mostly outside this region, apart from one reference tube located more centrally in the cavity near the tibia.

3.2 | Measured muscle concentration dependence on reference tube position

Table 1 gives the range of Na concentrations measured in the 2 volunteers per muscle group when using reference tubes 1–8. For the central tube, the concentration and SD over the four repeated measurements are also shown. For both volunteers, the measured NaCl concentration in a muscle depended greatly on the position of the reference tube, with a range of up 10 mM (Table 1, GM, volunteer 1). Before correction, the largest concentration was measured in the GM (volunteer 1: 26.3 mM volunteer 2: 23.6 mM) and smallest in the TA muscle (vol 1: 11.1 mM vol 2:11.1 mM). For all 10 tubes, the SD

TABLE 1 Measured NaCl concentrations in six muscle groups for the 2 volunteers

	Volunteer 1				Volunteer 2	
	Uncorrected		Corrected using normalized intensity map		Uncorrected	
Tissue region	Range tubes 1–8 (mM)	Central tube (mM) (SD)	Range tubes 1–8 (mM)	Central tube (mM) (SD)	Range tubes 1–8 (mM)	Central tube (mM) (SD)
TA	11.1–17.3	14.3 (0.7)*	12.9–15.2	14.6 (0.8)	11.1–16.6	14.4 (0.5)
EXT	13.1–20.3	16.9 (1.3)	15.2–17.9	17.2 (1.4)	12.8–19.0	16.5 (0.5)
TP	12.1–18.8	15.6 (0.5)	14.1–16.5	15.9 (0.6)	13.4–19.9	17.2 (0.2)
FBL	12.6–19.6	16.3 (0.8)	14.6–17.2	16.6 (0.8)	14.4–21.5	18.6 (0.7)
SOL	13.9–21.6	17.9 (0.8)	16.1–18.9	18.2 (0.8)	14.6–21.7	18.9 (0.6)
GM	16.9–26.3	21.8 (1.1)	19.6–23.1	22.2 (1.1)	15.9–23.6	20.5 (1.1)

Abbreviations: EXT, extensor longus; FBL, fibularis; GM, gastrocnemius medialis; NaCl, sodium chloride; SD, standard deviation; SOL, soleus; TA, tibialis anterior; TP, tibialis posterior.

*() – SD over the mean of the four repeated measurements.

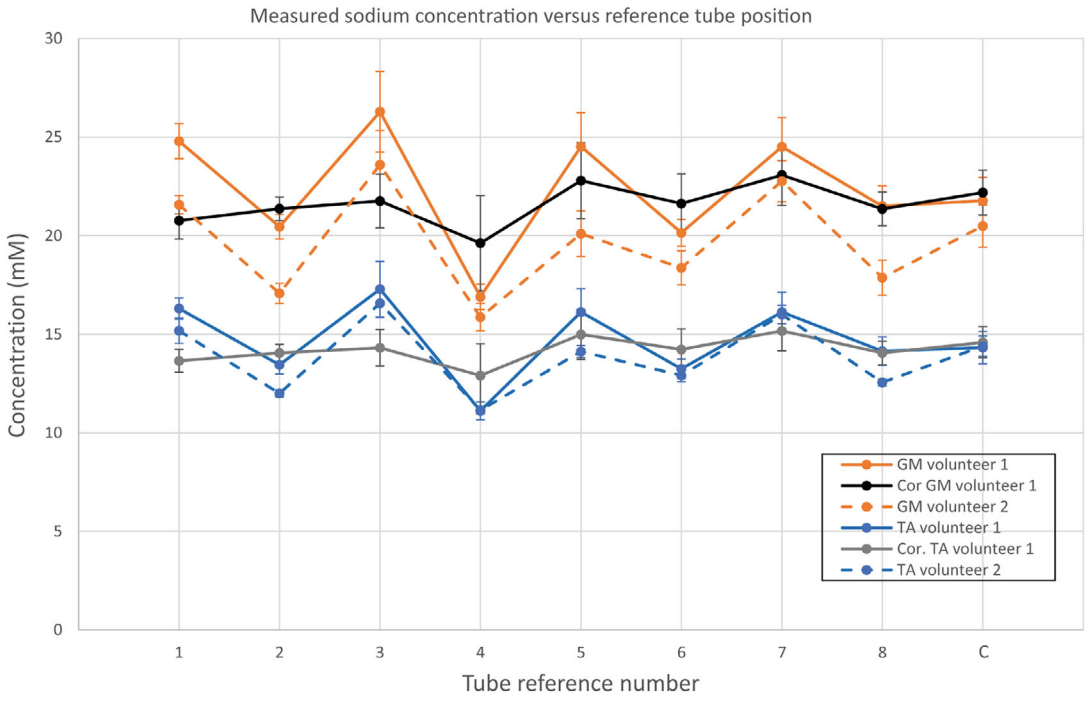

FIGURE 2 The measured concentration before correction in GM (orange line) and TA (blue line) muscles versus tube reference number (see Figure 1(C)) for volunteer 1 (solid line) and volunteer 2 (broken line). The solid black and gray lines illustrate the concentration values obtained after correction using a normalized intensity map for the GM and TA muscle group of volunteer 1, respectively. GM, gastrocnemius medialis; TA, tibialis anterior.

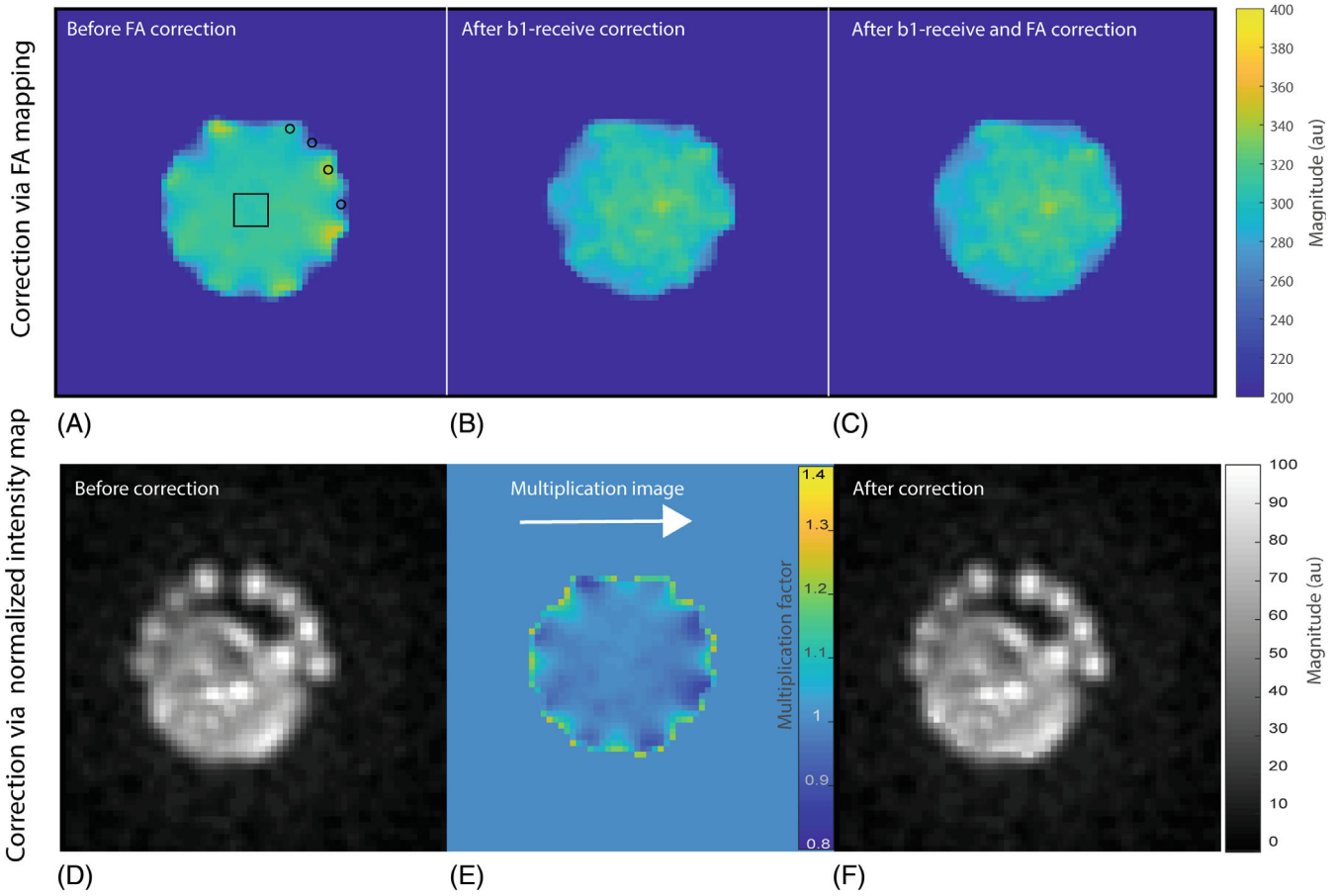

FIGURE 3 Top row: Correction in a phantom via FA mapping. (A) UTE (FA = 90°) magnitude image of a homogeneous phantom before and (B) after B_1-receive correction. (C) Magnitude image after B_1-receive and FA correction. The circles in (A) indicate the points evaluated. Bottom row: Correction using a normalized intensity map. (D) UTE (FA = 90°) in vivo magnitude image before correction. *(E) Phantom multiplication correction factor and (F) resulting magnitude image after correction. FA, flip angle.

over the four repeated measurements ranged from 0.2 to 2.2 mM.

Figure 2 further illustrates the measured concentration dependence on the reference tube position. As shown in Figure 1(C), tubes 1–4 contained 20 mM NaCl but were shifted in position, that is, at the same distance from the isocenter of the coil with increments of about 25°, and tubes 5–8; C contained 30 mM NaCl and shifted similarly in position. The GM and TA values alternated up and down from tube to adjacent tube location. The measured concentration using the central tube had a value close (< 1 mM) to the center value of the range measured by the other (nr 1–8) tubes.

The higher Na signals in tubes 2, 4, 6, and 8 are illustrated by the spectral map shown in Figure 1(D). In the shown chemical shift range of six ppm, intense peaks are seen in those voxels that give the best match with the tube positions, compared with weaker signals in voxels suffering from partial volume effects. Note also that in the muscles the Na peaks are broadened and a couple of ppm's shifted downfield relative to the reference tubes.

3.3 | Correction in a phantom using a normalized FA map

Figure 3(A) shows the magnitude image before correction. The B_1-receive correction (Figure 3(B)) appears to reduce the intensity inhomogeneity along the edge of the phantom. This inhomogeneity is further reduced after FA correction (Figure 3(C)) Although the corrected image appears more homogenous around the edge, the center of the phantom appears to have a higher intensity than toward edge of the phantom.

For all evaluated points (Figure 4(A)), the correction resulted in an intensity percent closer to 100%, with the exception of reference tube eight. The percent mean (± SD) of the four points before and after correction was 93.0% (±14.9%) and 92.2% (±5.0%), respectively. For the central

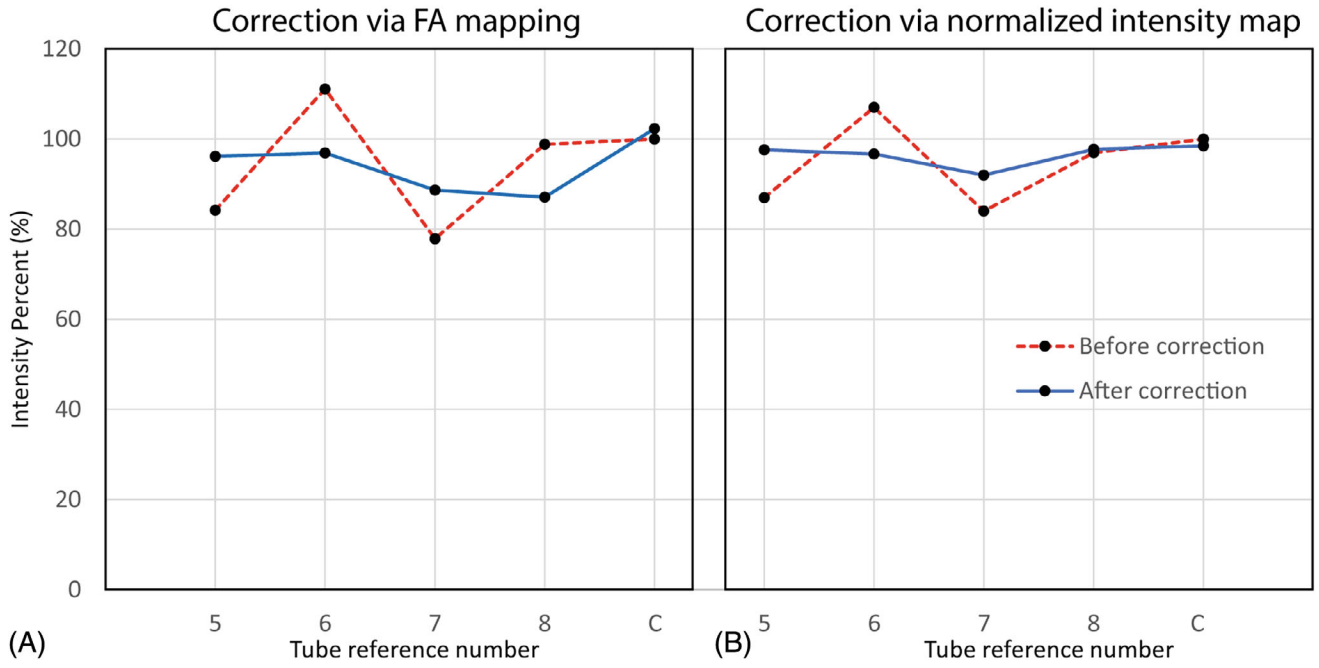

FIGURE 4 Intensity percent before (red line) and after (blue line) correction with respect to the more central tube/or location before correction (C, defined as 100%) (A) Correction in a phantom via FA mapping. (B) Correction of an in vivo scan using a normalized intensity map.

region, assumed not to be influenced by coil B_1 inhomogeniety, the correction resulted in a percent decrease of 1.5%.

3.4 | Correction using a normalized intensity map

Figure 3(D–F) shows the UTE image before and after correction using a normalized intensity map. Table 1 shows the range of concentration values obtain after correction for volunteer 1. The average reference tube-dependent range over all muscle groups decreased from 7.4 (1.1) mM before correction to 2.8 (0.5) mM after correction. In Figure 2(D), the solid black and gray lines illustrate the correction method applied to the GM and TA muscle group of volunteer 1, respectively. Using the reference tubes containing the 20 mM NaCl resulted in a lower calculated concentration of about 1.5 mM compared to the 30 mM NaCl tubes.

For all reference tubes evaluated (Figure 4(B)), the intensity percentage was closer to 100% after correction. The percent mean (±SD) of the four reference tubes before and after correction was 93.8% (±10.4%) and 96.0% (±2.7%), respectively. For the more central tube, assumed not to be influenced by coil B_1 inhomogeniety, the correction resulted in a percent increase of 2.3%.

4 | DISCUSSION

Our study has shown the importance of considering coil B_1 inhomogeneity for quantitative MR Na mapping of calf muscles, even when using a birdcage coil design. Depending on the reference tube location, we found a potential variation in the muscle measurement of up to 10 mM Na. Having coils as close as possible to the tissue of interest being scanned has SNR advantages, especially useful for Na imaging, but this study has shown that there is potential for large errors if this results in placement of the reference tubes close to the surface of the coil. Our results substantiate a suggestion that an elevated signal may result from the tissue being too close to the active RF coil rather than reflect true pathology.[14]

We explored two possible correction methods. The first based on FA mapping. As can be seen in Figure 3(C), this did result in a more homogenous intensity profile along the edge of the phantom. However, there remained a clear intensity offset at the edge region with the respect to the center region of about 8% (Figure 3(A)). This large offset remained, despite the correction being applied to a homogenous spherical phantom.

In addition, we investigated a correction via use of a homogenous phantom scanned, which was applied to the in vivo scans. Similar to the FA correction method, this resulted in less variation in intensity between the tubes (SD from 10.4% to 2.7%); however, a mean offset compared

to the central tube still remained of about 4%. Although we used the phantom correction method with the in vivo tubes positioned in a region of maximum and minimum B_1 inhomogeneity, it could be more challenging to do this in practice. It would require reference tubes fixed to the coil—and acquired for both phantom and in vivo scans so that image registration could be used to overlap in vivo and phantom images.

The correction methods had little influence (< 2%) (Figure 4, tube C) on the intensity value for the reference tube placed more centrally, and away from the surface coil (Figure 1C). This setup will therefore likely give the best quantification results.

Our study has several limitations. Firstly only two volunteers were scanned. However, these volunteers gave similar results (Figure 2) that were sufficient to show the large impact coil B_1 inhomogeneity may have on Na quantification in the calf muscles. Also, various coil sensitivity correction methods were not investigated. This includes the method based on calculating the coil sensitivity by acquiring an image with the same contrast using body coil and local coil.[22] This was not possible in our case because of RF shielding of the transmit–receive birdcage coil. Also, we did not investigate obtaining sensitivity maps using a low-pass filter,[23] which would be interesting future work. Lastly, a dual-tuned knee coil gives better shimming and ^{1}H imaging compared with a body coil at the cost of lower SNR in the Na signal as compared with a single tuned coil.

5 | CONCLUSIONS

The main aim of this study was to investigate the reliability of Na quantification in the calf muscle using a birdcage coil at 3T. This is important prior work for future clinical studies that will involve Na quantification of the calf muscle. We found large quantification errors with a range of up to 10 mM Na, and conclude that the more centrally located reference tube gives the most reliable quantification results.

ORCID

Paul Baron https://orcid.org/0000-0001-7408-2879

REFERENCES

1. Rose B, Post T, Narins RG. *Clinical Physiology of Acid Base Electrolyte Disorders*. McGraw-Hill Education; 2001.
2. Ouwerkerk R, Bleich KB, Gillen JS, Pomper MG, Bottomley PA. Tissue sodium concentration in human brain tumors as measured with Na-23 MR imaging. *Radiology*. 2003;227:529-537.
3. Inglese M, Madelin G, Oesingmann N, et al. Brain tissue sodium concentration in multiple sclerosis: a sodium imaging study at 3 Tesla. *Brain*. 2010;133:847-857.
4. Wheaton AJ, Borthakur A, Shapiro EM, et al. Proteoglycan loss in human knee cartilage: quantitation with sodium MR imaging-feasibility study. *Radiology*. 2004;231:900-905.
5. Maril N, Rosen Y, Reynolds GH, Ivanishev A, Ngo L, Lenkinski RE. Sodium MRI of the human kidney at 3 Tesla. *Magn Reson Med*. 2006;56:1229-1234.
6. Kopp C, Linz P, Dahlmann A, et al. 23Na magnetic resonance imaging-determined tissue sodium in healthy subjects and hypertensive patients. *Hypertension*. 2013;61:635-640.
7. Kopp C, Linz P, Maier C, et al. Elevated tissue sodium deposition in patients with type 2 diabetes on hemodialysis detected by (23)Na magnetic resonance imaging. *Kidney Int*. 2018;93:1191-1197.
8. Nagel AM, Amarteifio E, Lehmann-Horn F, et al. 3 Tesla sodium inversion recovery magnetic resonance imaging allows for improved visualization of intracellular sodium content changes in muscular channelopathies. *Invest Radiol*. 2011;46:759-766.
9. Hammon M, Grossmann S, Linz P, et al. 3 Tesla (23)Na magnetic resonance imaging during aerobic and anaerobic exercise. *Acad Radiol*. 2015;22:1181-1190.
10. Gerhalter T, Gast LV, Marty B, et al. Assessing the variability of Na-23 MRI in skeletal muscle tissue: reproducibility and repeatability of tissue sodium concentration measurements in the lower leg at 3 T. *NMR Biomed*. 2020;33:e4279.
11. Alhulail AA, Xia PY, Shen X, et al. Fast in vivo Na-23 imaging and T-2* mapping using accelerated 2D-FID UTE magnetic resonance spectroscopic imaging at 3 T: proof of concept and reliability study. *Magn Reson Med*. 2021;85:1783-1794.
12. Hayes CE, Edelstein WA, Schenck JF, Mueller OM, Eash M. An efficient, highly homogeneous radiofrequency coil for whole-body NMR imaging at 1.5-T. *J Magn Reson*. 1985;63:622-628.
13. Madelin G, Regatte RR. Biomedical applications of sodium MRI in vivo. *J Magn Reson Imaging*. 2013;38:511-529.
14. Nielles-Vallespin S, Weber MA, Bock M, et al. 3D radial projection technique with ultrashort echo times for sodium MRI: clinical applications in human brain and skeletal muscle. *Magn Reson Med*. 2007;57:74-81.
15. Nagel AM, Laun FB, Weber MA, Matthies C, Semmler W, Schad LR. Sodium MRI using a density-adapted 3D radial acquisition technique. *Magn Reson Med*. 2009;62:1565-1573.
16. Cunningham CH, Pauly JM, Nayak KS. Saturated double-angle method for rapid B1+ mapping. *Magn Reson Med*. 2006;55:1326-1333.
17. Madelin G, Jerschow A, Regatte RR. Sodium relaxation times in the knee joint in vivo at 7T. *NMR Biomed*. 2012;25:530-537.
18. Constantinides CD, Gillen JS, Boada FE, Pomper MG, Bottomley PA. Human skeletal muscle: sodium MR imaging and quantification-potential applications in exercise and disease. *Radiology*. 2000;216:559-568.
19. Fedorov A, Beichel R, Kalpathy-Cramer J, et al. 3D slicer as an image computing platform for the quantitative imaging network. *Magn Reson Imaging*. 2012;30:1323-1341.
20. Wang J, Mao W, Qiu M, Smith MB, Constable RT. Factors influencing flip angle mapping in MRI: RF pulse shape, slice-select gradients, off-resonance excitation, and B0 inhomogeneities. *Magn Reson Med*. 2006;56:463-468.
21. Vaidya MV, Collins CM, Sodickson DK, Brown R, Wiggins GC, Lattanzi R. Dependence of B1+ and B1- field patterns of surface

coils on the electrical properties of the sample and the MR operating frequency. *Concepts Magn Reson Part B Magn Reson Eng*. 2016;46:25-40.
22. Brey WW, Narayana PA. Correction for intensity falloff in surface coil magnetic resonance imaging. *Med Phys*. 1988;15:241-245.
23. Lachner S, Ruck L, Niesporek SC, et al. Comparison of optimized intensity correction methods for Na-23 MRI of the human brain using a 32-channel phased array coil a 7 Tesla. *Z Med Phys*. 2020;30:104-115.

How to cite this article: Baron P, Potze JH, Sijens PE. Influence of reference tube location on the measured sodium concentrations in calf muscles using a birdcage coil at 3T. *Magn Reson Med*. 2023;90:624-632. doi: 10.1002/mrm.29670